Sedimentary deposits of the 2011 Tōhoku-oki and A.D. 869 Jōgan tsunami events on the Sendai coastal plain, Japan

Jessica E. Pilarczyk[1,2*], Benjamin P. Horton[1], Robert C. Witter[3], Christopher H. Vane[4], Catherine Chagué-Goff[2,5], James Goff[2]

1. Sea Level Research, Department of Earth and Environmental Science, University of Pennsylvania, 240 S. 33rd Street, Philadelphia, PA 19104-6316, USA
Tel: +1 215 573-5145
Email: jpilar@sas.upenn.edu (J. E. Pilarczyk), bphorton@sas.upenn.edu (B. P. Horton)

2. Australia-Pacific Tsunami Research Centre, School of Biological, Earth and Environmental Sciences, University of New South Wales, Sydney 2052, Australia
Tel: +612 9385 8431
Email: jpilar@sas.upenn.edu (J. E. Pilarczyk), c.chague-goff@unsw.edu.au (C. Chague-Goff), j.goff@unsw.edu.au (J. Goff)

3. United States Geological Survey/Alaska Science Center, Anchorage, AK 99508, USA
Tel: +1 907 786-7404
Email: rwitter@usgs.gov (R. C. Witter)

4. British Geological Survey, Keyworth, Nottingham, U.K NG125GG
Tel: +44 (0) 115 936 3017
Email: chv@bgs.ac.uk (C. H. Vane)

5. Australian Nuclear Science and Technology Organisation, Locked Bag 2001,
Kirrawee DC, NSW 2232, Australia
Email: ccg@ansto.gov.au (C. Chague-Goff)

*Corresponding Author
Jessica E. Pilarczyk
Sea Level Research, Department of Earth and Environmental Science, University of Pennsylvania, 240 S. 33rd Street, Philadelphia, PA 19104-6316, USA
1280 Main Street West, Hamilton, Ontario, Canada, L8S 4K1
Tel: +1 215 573-5145
Email: jpilar@sas.upenn.edu (J. E. Pilarczyk)

Abstract

The 2011 Tōhoku-oki megathrust earthquake (Mw 9.0) generated a tsunami that reached the Sendai coastal plain with wave heights of ~10 to 12 m above sea level. In May 2011 we examined the tsunami deposit exposed in 14 shallow trenches along a ~4.5 km transect perpendicular to the coast on the northern perimeter of the Sendai airport (38.145°N, 140.933°E). We document the stratigraphical, sedimentological, foraminiferal and geochemical characteristics of the Tōhoku-oki tsunami deposit and compare these to sediments deposited by the Jōgan tsunami of A.D. 869.

In rice fields inundated by the Tōhoku-oki tsunami, a poorly-sorted, dark brown agricultural soil is buried by a poorly-sorted, brown, medium-grained sand-sheet. In trenches located more than 1.2 km inland, the sand is capped by a 2 cm thick mud. The tsunami deposit is thickest (30 cm) near the coastal dune and its sheet-like geometry thins to less than 5 cm thick ~4.5 km inland. The tsunami deposit was discriminated from the underlying soil by the sudden appearance of recent and fossil foraminifera and a pronounced increase in grain size that fined upwards and landwards. The recent foraminifera preserved in the sandy facies of the deposit are low in number and showed evidence of prolonged subaerial exposure (e.g. pitting, corrosion, fragmentation). The recent foraminifera likely originated from coastal dune and beach sediments that were breached by the tsunami. In contrast, there were high abundances of robust, sediment in-filled fossil foraminifera in the tsunami deposit that have probably been eroded from coastal Triassic-Jurassic sandstone headlands north of Sendai. Trends associated with test size (e.g. decreasing concentration of large test sizes with distance inland) are in agreement with grain size data. Geochemistry revealed a decrease in total organic carbon and an increase in $\delta^{13}C$ in the tsunami sand compared to the underlying soil, supporting a marine origin for the upper unit.

The Jōgan and Tōhoku-oki deposits show many similarities. The Jōgan deposit consists of medium sand that sharply overlies a finer grained sandy soil; however, the absence of a mud cap and internal sedimentary structures indicates post-depositional change. The tsunami deposit contains similar fossil foraminifera, but with the presence of recent planktic species, which were not found in overlying or underlying sedimentary

units.

1. Introduction:

Records of past tsunamis developed from the sedimentary evidence they leave behind, improve our understanding of the frequency of tsunamis by expanding the age range of events available for study (Morton et al., 2007). Proper hazard assessment depends on an awareness of tsunamis and their impacts on coastal geomorphology, ecology and rapidly expanding coastal populations. Stratigraphical sequences of tsunami deposits are often used to estimate recurrence intervals and provide insight into their source (e.g. earthquakes, landslides, volcanic eruptions; Bernard and Robinson, 2009). Reconstructions have shown repeated tsunamis during the Holocene in the Pacific northwest (Kelsey at al., 2005), North Sea (Bondevik et al., 2005), New Zealand (Goff et al., 2001) and Kamchatka (Pinegina et al., 2003), and in the regions of the 1960 Chile (Cisternas et al., 2005) and 2004 Indian Ocean (Jankaew et al., 2008) earthquakes.

Identification of tsunami deposits is often based on recognition of anomalous sand-sheets in low-energy environments such as coastal ponds, lakes, and marshes, which can be supported by microfossil evidence. For example, the A.D. 1700 Cascadia tsunami can be identified with confidence from a sand unit that tapers landward (often for several kilometres), contains a mixed microfossil assemblage and coincides with stratigraphical evidence for abrupt coseimic subsidence (e.g. Hawkes et al., 2011). Foraminiferal taxonomy has been commonly used as an indicator of tsunami deposits (e.g. Mamo et al., 2009) and most taphonomic studies of foraminifera focus on time-averaging or lateral transport of tests with only semi-quantitative observations on test condition (e.g. Hawkes et al., 2007; Kortekaas and Dawson, 2007; Uchida et al., 2010). Recent research has shown that test condition provides further information regarding energy regimes and transport history (e.g. Hawkes et al., 2007; Kortekaas and Dawson, 2007; Uchida et al., 2010; Pilarczyk and Reinhardt, 2011, 2012; Pilarczyk et al., 2011).

The proxy toolkit to examine paleo-tsunamis has expanded following the modern surveys on the 2004 Indian Ocean and 2009 South Pacific tsunamis (Chagué-Goff et al., 2011). New possible techniques such as geochemistry can provide evidence for marine inundation and high-energy flows (Szczuciński et al., 2005; Chagué-Goff, 2010; Chagué-Goff et al., 2011). In this study we document the utility of geochemistry, together with the more established foraminifera (taxa and taphonomy) and sedimentology (grain size), as indicators of the 11 March 2011 Tōhoku-oki tsunami deposit. We compare this deposit with an older event of similar magnitude, the A.D. 869 Jōgan tsunami (Fig. 1).

1.1 2011 Tōhoku-oki tsunami

On 11th March 2011 a great megathrust earthquake (Mw 9.0) along the Japan Trench generated a tsunami that reached the Sendai Plain on the northeastern coast of Honshu, Japan (Fig. 1a) at 14:46 (Japan Standard Time) with run-up heights of 10 – 40 m (Sugawara et al., 2011a). The earthquake ruptured over a distance of ~400 km with upwards of 5 m vertical and 24 - 60 m lateral displacement of the seafloor (Ito et al., 2011; Sato et al., 2011). The low-lying configuration of the coastal plain made Sendai particularly susceptible to tsunami inundation that reached 4.5 km inland in some areas (Sugawara et al., 2011a). Sustained flooding several months after the event was documented at several locations along the Sendai Plain (Sugawara et al., 2011a). We conducted a field survey north of the Sendai airport (Fig. 1a) and found evidence of inundation heights of 10 to 12 m above Tokyo Peil (TP; mean sea level in Tokyo Bay) behind artificially emplaced dunes (Fig. 2). Approximately 2 km from the shoreline, inundation heights were noted to be 3 – 4 m above TP, and ~20 cm at a distance of 4 km from the shoreline. The hardest hit area was at a distance of 0 – 2.5 km from the shoreline where houses and roads were severely damaged and rice fields flooded with saltwater. Goto et al. (2011) reported 17 – 21 cm of co-seismic subsidence approximately 10 km south of the Sendai airport and earthquake-induced liquefaction in the adjacent rice fields.

1.2 A.D. 869 Jōgan tsunami

Predecessors of the Tōhoku-oki tsunami (A.D. 1611 Keichō, A.D. 1793 Kansei, A.D. 1896 Meiji Sanriku, A.D. 1933 Shoa Sanriku, A.D. 1978) are numerous (Miyagi-oki; Minoura and Nakaya, 1991; Minoura et al., 2001; Sawai et al., 2008a,b). However, only the Jōgan tsunami in A.D. 869 approaches the 2011 tsunami in terms of its magnitude, area of coastline impacted (Sendai and Sōma regions) and extent of inundation (greater than 2 km inland). On 13 July A.D. 869 an offshore earthquake approximately 200 km from the Sendai coastal plain resulted in a large-scale tsunami with widespread flooding (Fig. 1a). Estimates of the magnitude of the earthquake that generated the Jōgan tsunami, as well as flow depths and inundation distances have been investigated to improve tsunami hazard assessments (e.g. Zhao et al., 1990; Satake et al., 2008; Sugawara et al., 2011b).

The Jōgan deposit is a landward-thinning, laterally extensive sand unit of variable thickness (~2 – 20 cm) that extends over the Sendai and Sōma regions (Sawai et al., 2008a; Sugawara and Imamura, 2010). The deposit consists of well-sorted medium sand intercalated with terrestrial organic-rich mud (Minoura et al., 2001). Overlying the Jōgan deposit is a thin soil unit that is capped by the grayish-white felsic Towada-a tephra emplaced by a volcanic eruption to the northeast of Sendai in A.D. 870-934 (Yamada and Shoji, 1981; Minoura et al., 2001). Abundant marine and brackish water diatoms have been documented within the deposit (Minoura et al., 2001), but foraminifera have not been studied. The tsunami deposit extends 2.8 km inland, however, since the Sendai Plain coastline has prograded 1 km over the last ~1000 years, the inland extent of the Jōgan deposit is now ~4 km inland (Sawai et al., 2008b; Sugawara et al., 2011b).

2. Regional setting:

The Sendai Plain is a low-lying (less than 5 m TP), wave-dominated, microtidal (mean tidal range of ~1 m) coastal plain, which extends approximately 50 km on the Pacific coast of north-eastern Japan (Fig. 1a). The area is bounded by hills to the north, west and south, and a steep continental shelf gradient (Tamura and Masuda, 2004, 2005). Mid-Pleistoncene marine and non-marine sediments dominate the coastal plain with Jurassic – Holocene marine and non-marine sedimentary rock outcropping to the north (Geological Survey of Japan, 2009). The Sendai Plain supports rice cultivation, with many fields interspersed with low-density housing (Fig. 1b). Main sediment sources to the area include three rivers (Abukuma, Natori and Nanakita rivers) that account for the continued seaward progradation of the coastline since the mid-Holocene (Saito, 1991; Tamura and Masuda, 2005).

Our study area (near Sendai airport) has four environments: coastal; coastal forest; paved landscape; and rice fields. The coastal zone transitions from nearshore marine (-0.8 m TP) to beach (1.7 m TP) to artificial dune (2.3 m TP; Fig. 1b; Fig. 2; Fig. 3a) within a distance of ~0.5 km from the shoreline. The artificial dune is composed of allochthanous sediment that was brought in to armor the coastline (Fig. 2a). We do not know the origin of the dune sediment, but noted its difference in color and composition to adjacent beach and nearshore marine sediment. The coastal forest (Fig. 1b, 2b), sitting at a distance of ~0.2 km from the coastline and an elevation of ~2.3 m TP), consists of mature pine trees that were planted 300 years ago as a means of protecting rice fields from salt spray (Sugawara and Imamura, 2010). Directly landward of the coastal forest is a paved landscape that contains several reinforced canals (0.1 – 1.2 km from coastline, ~1 m TP), and rice fields (1.2 – 4.5 km from coastline, -0.4 – 1.2 km TP).

3. Methods:

3.1 Sample collection, stratigraphy and geomorphology of the Tōhoku-oki tsunami deposit

In May 2011 we examined 14 trenches (Fig. 1b; Fig. 3a) containing the Tōhoku-oki tsunami deposit and its underlying soil along a transect from the coastal forest (trenches 5 - 9; 0.3 - 0.4 km inland), paved landscape (trenches 12 - 24; 0.4 - 1.2 km inland) and rice fields (trenches 31 - 86; 1.2 - 4.5 km inland). The trenches were sampled (2 – 10 cm resolution) and described in terms of deposit thickness and sedimentological composition. We examined each of the 14 trenches for lateral changes (average of all samples obtained in the tsunami deposit) associated with increasing distance inland and selected six sections for detailed analysis of vertical changes of the tsunami deposit with depth (e.g. trenches 5, 12, 31, 36, 48, 86). We used a node at the shoreline to calculate the distance of each surface sample and trench location relative to the marine source. In addition we collected surface samples (upper 1 cm) spanning the entire coastal zone (sites 1 - 4; -0.1 - 0.3 km inland) for comparison with tsunami sediments.

3.2 Grain size analysis

We conducted grain size analysis using a Beckman Coulter laser diffraction particle size analyzer on all surface and trench samples. Prior to analysis, organics were removed and samples were stirred as a moist paste to homogenize the sediment and disaggregated with sodium hexametaphosphate following the methods of Donato et al. (2009). Grain size values for all surface samples and 14 trench sections were converted to the Wentworth-Phi Scale, interpolated and gridded using a Triangular Irregular Network (TIN) algorithm according to Sambridge et al. (1995), and plotted as Particle Size Distributions (PSDs) in Geosoft Oasis TM. We used a Camsizer to calculate particle size sphericity ranging from 0 (highly angular) to 1 (perfectly spherical). Grain size descriptions follow Folk (1974)

3.3 Foraminiferal analysis

We conducted foraminferal analysis on all surface and trench samples following the methods of Horton and Edwards (2006) where approximately 5 cm^3 samples were sieved (>63 μm) and examined in a liquid medium. Taxonomy followed Loeblich and Tappan (1987) and Hayward et al. (2004), and where possible, we counted up to 300 recent specimens. Since we found no agglutinated species, samples were then dried at 25°C, sieved and recorded as having small (<250 μm) or large (>250 μm) test sizes. We categorized individual specimens as recent (white; late Holocene) or fossil (robust, sediment in-filled and calcified; Triassic-Jurassic); after Pilarczyk et al., 2011; Plate 1). Fossil foraminifera are easily identified since they generally maintain their test structure even after wave agitation disaggregates them from their parent rock. However, residence time in the nearshore environment results in significant abrasion and obscuring of diagnostic test features (e.g. aperture, perforations, umbo, etc.) required for proper species identification. Total number of individuals (fossil and recent individuals combined), total recent, total fossil and percent large specimens were enumerated.

3.4 Geochemical analysis

For measurement of $\delta^{13}C$ and total organic carbon (TOC) in trenches, we selected two trenches (5 and 31), which include the soil, overlying sand and mud cap. Sediment samples were treated with 5% HCl for 18 hours, washed with deionised water, dried in an oven at 40ºC overnight and milled to a fine powder using a pestel and mortar. Plant samples were treated with 5% HCl for 2 - 3 hours, washed with deionised water, dried in an oven at 40ºC overnight and milled to a fine powder using a freezer mill. $^{13}C/^{12}C$ analyses were performed on sediment samples by combustion in a Costech Elemental Analyser coupled on-line to an Optima dual-inlet mass spectrometer. $\delta^{13}C$ values were calculated to the VPDB scale using a within-run laboratory standard (cellulose, Sigma Chemical prod. no. C-6413) calibrated against NBS-19 and NBS-22. Organic carbon values (TOC wt/wt) were analysed on the same instrument. Replicate analysis indicated a precision of <0.1‰ (1 SD) for $\delta^{13}C$ and 0.1% TOC (wt/wt) measurements. All sediments reported for geochemistry were sampled over a 1 cm increment and are plotted as an average depth. With the exception of the pine roots which have a %N of 0.6 and C/N of 85.3, the %N values were below the limit of detection (LOD) of ~0.1%, therefore C/N values were unavailable to distinguish local from imported organic matter.

3.5 Analysis of the A.D. 869 Jōgan tsunami deposit

We also logged and sampled a trench containing evidence of the A.D. 869 Jōgan tsunami in a rice field ~10 km north of the Tōhoku-oki transect (Fig. 1a). The Jōgan deposit has previously been documented (Minoura et al., 2001; Sawai et al., 2008a; Goto et al., 2011). We logged the section in the field and conducted foraminiferal and grain size analysis as outlined in sections 3.2 and 3.3.

4. Results:

The tsunami deposited a sand-sheet that was laterally extensive and reached distances in excess of 4.5 km from the coast (Fig. 3). Erosion was severe where the tsunami breached an artificially emplaced and reinforced dune system and flattened trees in the coastal forest. Field descriptions of the tsunami deposit document a landward thinning and texturally fining sandy deposit. In some trenches, the sand-sheet was laminated with alternating sand and heavy mineral laminae (e.g. trench 31; Fig. 2c). Small mollusk fragments were present in very minor amounts (<1%) in nearshore and beach samples but not in the tsunami deposit.

4.1 Surface sediments

Grain size results distinguished between intertidal (nearshore; beach; sites 1, 2, 3) and dune (site 4) surface samples (Fig. 3). We found coastal sediments (sites 1 to 4) to have similar grain sizes (mean = 0.8φ ± 0.3), but varying degrees of sorting (StD = 2.5φ ± 0.8) and sphericity (0.6 ± 0.3). Nearshore sediment (mean = 0.9φ ± 0.6), with the lowest sphericity values (0.4 ± 0.1, with 1.0 being a perfect sphere), was most angular in composition, followed by beach (mean = 0.6 φ; sphericity = 0.8) and artificial dune sediment (mean = 0.9 φ; sphericity = 0.9), which were significantly more rounded in grain composition.

Surface sediment samples also showed distinctly different foraminiferal characteristics that relate to increasing distance away from the marine source. Nearshore marine samples (sites 1 and 2) had the lowest concentration of recent individuals per cm^3 (9 ± 1), the highest concentration of fossils (124 ± 18) and the greatest abundance of large fossil specimens (59% ± 3). The artificial dune (site 4) was characterized by the lowest concentration of fossils (19 individuals per cm^3), but the highest concentration of recent foraminifera (77 individuals per cm^3), which were comparatively small in size (only 45% of fossils were >250 µm). Beach sediment (site 3) marked a transition zone and had intermediate concentrations (fossil concentration = 90 individuals per cm^3; recent concentration = 2 individuals per cm^3; % large fossils = 50%).

4.2 Lateral changes within the Tōhoku-oki tsunami deposit

The tsunami deposit showed trends with increasing distance inland (Fig. 3e-i). In general, sediments become finer grained (1.0φ ± 0.5 at 0.3 km; 1.6 φ ± 0.1 at 3.0 km; 2.1φ ± 0.0 at 4.5 km), less sorted (2.3φ ± 0.7 at 0.3 km; 2.2 φ ± 0.1 at 3.0 km; 1.6φ ±

0.2 at 4.5 km) and more angular (0.7 ± 0.1 at 0.3 km; 0.3 ± 0.1 at 3.0 km; 0.4 ± 0.0 at 3.7 km) with increasing distance inland. The deposit thickness also thinned from 25 cm at a distance of 1 km from the shoreline to <5 cm at 4.5 km.

The tsunami deposit contained a combination of recent (e.g. calcareous, late Holocene) and fossil (sediment in-filled, Triassic-Jurassic) foraminifera. Recent foraminifera were taphonomically altered showing signs of significant fragmentation, edge rounding (abrasion) and dissolution. Fractured edges also showed evidence of edge rounding indicating fragmentation occurred before tsunami deposition. Taphonomic alteration prevented proper species identification except *Ammonia parkinsoniana*, which was present in most samples, although in very low abundances (<20 individuals per 1 cm^3). Miliolids were also found in low abundances. Analyses of the trench sections versus distance inland showed analogous relations to the surface samples regarding the abundances of fossil and recent foraminifera. Recent individuals, although low in abundance, peaked at trenches 5 (25 ± 8 individuals per cm^3) and 12 (29 ± 11 individuals per cm^3) and decreased by ~50% by trench 48 (12 ± 7 individuals per cm^3). At the landward limit extent of our transect, 4.5 km, (trench 86) no recent foraminifera were found (Fig. 3c).

Fossil foraminifera were more robust, darker in color, highly abraded and much more abundant than recent specimens within the tsunami deposit in all trenches (Fig. 5). Abundances of fossil foraminifera within the tsunami deposit peak at trenches 9 and 12 (102 ± 76 individuals per cm^3, 104 ± 10 individuals per cm^3 respectively) immediately inland of the coastal forest (0.4 – 0.5 km inland), and decrease to less than 3 individuals per cm^3 by trench 86 (Fig. 3b). Similarly, large fossil individuals (>250 µm) dominate trenches between trench 12 (67%) and trench 31 (64%), rapidly decrease in abundance at trench 48 (24%) and are almost non-existent by trench 86 (<1%; Fig. 3d).

4.3 Vertical changes within the Tōhoku-oki tsunami deposit

The six trench sections (5, 12, 31, 36, 48, 86) are characterized by three distinct units (Fig. 4, 5, 6). Trenches had basal rice field soil with a pronounced orange-brown color, consisting of poorly-sorted to very poorly-sorted medium sand (mean = 1.4□ ±

0.2; mode = 1.2□ ± 0.0; StD = 2.0□ ± 0.3). This was sharply overlain with a medium grained sand-sheet (mean = 1.1□ ± 0.4; mode = 1.3□ ± 0.4; StD = 2.2□ ± 0.7) that transitioned into a mud cap (mean = 2.4□ ± 0.7; mode = 2.0□ ± 0.3; StD = 2.5□ ± 0.1). The mud cap was only found at sites greater than 1.2 km from the coastline. The sand-sheet and mud cap together comprise the tsunami deposit. The tsunami deposit generally fined upwards (e.g. trench 12: 0.5 □ at bottom of deposit, 0.8□ at middle, 1.2□ at top; trench 31: 0.6 □ at bottom, 1.1□ at middle, 1.6□ at top, 1.7□ at mud cap) and became less sorted (e.g. trench 12: 1.3□ at bottom, 1.5□ at middle, 2.7□ at top; trench 31: 1.2□ at bottom, 1.9□ at middle, 2.9□ at top, 2.6□ at mud cap), and in some cases (e.g. trench 31) contains finer dark laminae. Particle sphericity did not show any consistent vertical trends within the tsunami sands or between the tsunami sands and the mud cap; at trench 31 the mud cap is more angular (0.5) than the tsunami sand (0.7 ± 0.2); whereas at trench 48 the mud cap (0.6) is more rounded compared to the underlying sand (0.3 ± 0.0; Fig. 5).

Foraminifera (fossil and recent) are absent within the soil, except at trenches 5 and 31 where very low abundances (11 ± 0 recent and 65 ± 0 fossil individuals per cm^3 at trench 5; 3 ± 2 recent and 53 ± 25 fossil individuals per cm^3 at trench 31) are found near the contact with the overlying sand suggesting some bioturbation (Fig. 5). Foraminifera are present in the tsunami sand (19 ± 13 recent and 82 ± 29 fossil individuals per cm^3) and mud cap (8 ± 18 recent and 10 ± 15 fossil individuals per cm^3), with little or no variations in abundance with depth, except at trenches containing a mud cap where abundances of fossil specimens are significantly higher in the sand than in the mud cap. However, the proportion of large recent and fossil foraminifera were highest at the bottom of the tsunami deposit and showed a slight upwardly fining sequence in most trenches. For example, recent and fossil foraminifera at the base of the tsunami deposit at trench 12 were 63% and 71% large (>250 µm) respectively and decreased to 45% and 56% at the top of the unit. Test size grading was most pronounced in trenches containing mud caps (e.g. trench 31: 70% large sized fossils at the bottom of the tsunami unit, 50% at the top of the sand and 30% in the mud cap; 70% large sized recent foraminifera at the bottom, 49% at the top of the tsunami sand and 40% in the mud cap).

Geochemistry of two trench sections (5, 31) distinguished between the tsunami deposit and the underlying soil (Fig. 5). In trench 5, $\delta^{13}C$ ranged from -27.0 to -24.8‰ in the tsunami sand and from -29.5 to -30.8‰ in the soil. TOC values were notably low in the tsunami deposit (~0.1%) compared to the underlying soil (0.5 – 5.9%). Similar to grain size results, three distinct units are distinguished in the geochemical profile of trench 31. From 17.5 to 11.5 cm the soil has δ^{13}C values of –27.8‰ to -27.1‰ and TOC values ranging from 1.5 to 5.7%. The TOC decreases 0.1% and the δ^{13}C values increase to 26.3‰ in the tsunami sand. The tsunami mud cap shows slightly elevated TOC values (0.3%) and much higher δ^{13}C (-15.1‰).

4.4 A.D. 869 Jōgan tsunami deposit

The Jōgan trench consisted of four stratigraphic units (basal soil, Jōgan tsunami deposit, Towada-a tephra, and overlying soil; Fig. 4d), of which the bottom three were sampled and analyzed. The soil is composed of a very poorly-sorted (StD = 2.8□ ± 0.1) sandy soil (mean = 2.1□ ± 0.3). The overlying Jōgan tsunami deposit is a 10 cm thick very poorly-sorted (StD = 3.0□ ± 0.1), medium sand (mean = 1.6□ ± 0.0). The tsunami deposit is capped by the fine grained Towada-a tephra (mean = 2.6□; StD = 2.7□). The contacts between these three units were gradational. The Jōgan tsunami deposit showed similar trends as the Tōhoku-oki with respect to thickness and sedimentological characteristics: slight fining in grain size (1.5□ at 52 cm to 1.6 □ at 47 cm), better sorting (3.1□ at 52 cm to 3.0 □ at 47 cm), and greater particle sphericity (0.6 at 52 cm to 0.7 at 47 cm; Fig. 4) from the bottom of the deposit to the top. The Jōgan tsunami deposit showed a pronounced influx of highly spherical sediment (sphericity = 0.7 ± 0.0) compared to the surrounding Towada-a (0.3) and soil (0.3 ± 0.1; Fig. 3h; Fig. 5). In the modern environment, highly spherical sediments seem to be originating from the beach (0.9) and dunes (0.9). Unlike the Tōhoku-oki tsunami deposit, the Jōgan did not contain a mud cap or evidence of internal sedimentary structures (e.g. laminae).

Foraminifera were present (190 ± 2 recent and 162 ± 5 fossil individuals per cm^3) in the tsunami deposit indicating a marine origin. Low abundances of foraminifera were found in the upper samples of the basal soil (fossil = 42; recent = 65 individuals per cm^3) and the lower part of the Towada-a tephra (fossil = 3; recent = 16 individuals per cm^3) suggesting bioturbation. This is similar to basal soils underlying the Tōhoku-oki deposit (trenches 5, 31 and 48), where no recent or fossil foraminifera were found below the bioturbated contact (Fig. 5). The Towada-a tephra contained no fossil foraminifera and less than 40 recent individuals per cm^3. The recent foraminiferal assemblage of the Jōgan tsunami deposit consisted of *Ammonia parkinsonia*, various taphonomically altered miliolids and unaltered planktics; in contrast to the Tōhoku-oki deposit where no planktics were found. Compared to the Tōhoku-oki deposit, *Ammonia parkinsoniana* individuals were more altered, showing signs of increased abrasion and dissolution. Large test sizes dominate the tsunami deposit and do not appear to show evidence of grading.

5. Discussion:

5.1 Stratigraphy and grain size analyses of the 2011 Tōhoku-oki tsunami

Tsunami deposits of Hokkaido Japan (Sawai, 2002), New Zealand (Goff et al., 2001), Papua New Guinea (Morton et al., 2007), Cascadia (Hawkes et al., 2011), Oman (Donato et al., 2009; Pilarczyk and Reinhardt, 2012) and elsewhere have been described on the basis of their lateral, sheet-like geometry, with the deposit thickness tapering inland (Morton et al., 2007; Goff et al., 2011). At Sendai, the tsunami deposit was laterally extensive over a 4.6 km transect and tapered inland from 30 cm to less than 5 cm and contained finer dark laminae interbedded with sand at some trenches (trench 31). The Tōhoku-oki sand-sheet is similar in mean grain size (1.1□ ± 0.4) and degree of sorting (2.2□ ± 0.7) to surface nearshore (mean = 0.9□ ± 0.6; StD = 2.2□ ± 0.3), beach (mean = 0.6□; StD = 1.9 □) and dune (mean = 0.9 □; StD = 3.6 □) surface samples supporting the suggestion of Goto et al. (2011) who ascribe a nearshore to dune origin for the tsunami sand. The finer underlying rice field soil (mean = 1.4□ ± 0.2) sharply transitioned to a coarser sand-sheet (mean = 1.1□ ± 0.4) that fined upwards to a mud cap (mean = 2.4□ ± 0.7). This fining upwards sequence within tsunami deposits is in agreement with several other studies (e.g. Hawkes et al., 2007; Morton et al., 2007; Goodman-Tchernov et al., 2009) and represents entrainment of sediment from multiple locations (nearshore, dune, etc.) followed by rapid deposition. The mud layer that caps the sand-sheet at trenches located at least 1.5 km from the shoreline represents further waning energy and is likely derived from antecedent rice field soil, canal mud or deeper offshore mud. It is possible the tsunami scoured deeper offshore entraining finer grain sizes that were deposited in areas of sustained flooding. This interpretation is further supported by TOC, $\delta^{13}C$ and foraminiferal results which favor a marine origin for the mud cap.

5.2 Recent and fossil foraminifera as a tsunami indicator

The presence of abundant foraminifera is a characteristic of tsunami deposits (e.g. Hawkes et al., 2007; Kortekaas and Dawson, 2007; Mamo et al., 2009; Pilarczyk and Reinhardt, 2011; Pilarczyk and Reinhardt, 2012), but at Sendai their abundance within the sand-sheet and mud cap was very low. Hawkes et al. (2007) found up to 1,400 individuals per cm^3 in the 2004 Indian Ocean tsunami deposits in Malaysia and Thailand, whereas we only found up to 48 recent individual per cm^3. The lack of recent foraminifera within nearshore sediments is also anomalous when compared to studies from other Japanese coastlines (e.g. Toba, Mie Prefecture, Hokkaido) that report abundant and diverse assemblages (Okashashi et al., 2002; Nanayama and Shigeno (2004; 2006). Szczucinski et al. (this volume) also report a surprising distinct paucity of nannoliths (biogenic carbonate) in nearshore areas as well as the Tōhoku-oki tsunami deposit, suggesting water chemistry as a possible reason for the lack of carbonate material. Furthermore, the foraminifera within the tsunami deposit were highly taphonomically altered. Taxonomic identification was impossible except *Ammonia parkinsoniana*. *A. parkinsoniana* has previously been documented as inhabiting littoral (5 - 10 m deep) to sub-littoral (<300 m deep) areas in Hokkaido, Sanriku and Boso Penninsula, Japan (Takata et al., 2006; Uchida et al., 2010) and elsewhere (e.g.; Debenay et al., 1998;). *A. parkinsoniana* is found unaltered in nearshore marine sediment.

The taphonomic character of recent foraminifera has been successfully used as an overwash indicator in several studies, because it provides additional information concerning energy regimes and transport history (e.g. Uchida et al., 2010). Within the Tōhoku-oki tsunami deposit, recent foraminifera showed evidence of subaerial exposure through a high degree of abrasion (edge rounding), corrosion and fragmentation (Berkeley et al., 2009; Pilarczyk et al., 2011). Contrary to other taphonomic studies of tsunami sediments (e.g. Kortekaas and Dawson, 2007), fragmentation at Sendai was not a function of the tsunami. Rather, edge rounding of fractured surfaces indicates repeated subaerial exposure and significant residence time in the intertidal zone (beach and artificial dune). Abundances of recent foraminifera peak in modern dune samples and likely do not represent modern conditions at Sendai since artificial dune sediment was transported in from an unknown source.

In the absence of high numbers of recent foraminifera, fossil specimens were a reliable indicator. Fossil individuals are found in all trenches, including the landward limit of the transect (4.6 km), and show a marked decrease in concentration and size with increasing distance inland. It appears that fossil specimens are marine indicators, probably eroding from coastal Triassic-Jurassic sandstone headlands that are found north of our study area. Supporting this inference are the large (>250 µm) individuals, which are found in very high abundances exclusively in nearshore sediment. Both fossil and recent foraminifera showed trends with distance, where abundances declined with increasing distance inland. The abundance of large size individuals (e.g. >250µm) ranged from 60 – 70% between the coastline and 1.5 km inland where they markedly began to decrease to 30 – 35% at 2.5 km and finally to a negligible amount (e.g. <1%) at 4.5 km inland). The abrupt decrease in abundance of large size individuals at 1.5 km inland coincides with the beginning of the mud cap (e.g. trench 31 at 1.6 km and trench 48 at 2.4 km) and likely represents waning energy and sustained pooling of marine water.

5.3 Geochemical trends

Stable carbon isotopes ($\delta^{13}C$) and total organic carbon (TOC) have been used extensively to infer the provenance of organic matter hosted in terrestrial, coastal wetland and marine sediments (e.g. Tyson, 1995; Lamb et al., 2007; Vane et al., 2010; Kemp et al., 2011). Although $\delta^{13}C$ and TOC have the potential to distinguish tsunami sediment from underlying soils primarily because imported marine sands should have low TOC content and higher $\delta^{13}C$ values than the local terrestrial soils, they have yet to apply.

In trench 5, the rice field soil has low $\delta^{13}C$ values (-30.8‰) and TOC of up to 6%. Pine roots that are found in the soil have similar $\delta^{13}C$ (-30.4‰), which are consistent with values reported from other forest soils (e.g. Goni and Thomas, 2000; Vane et al., 2003; Goni and Eglinton, 1996). This suggests a woody terrestrial plant material source for the rice field soil. In contrast the overlying tsunami sand has $\delta^{13}C$ values ranging from -27.0 to -24.8‰ and very low TOC of about 0.1% (Fig. 5). The $\delta^{13}C$ of marine and open coastal sediments typically range between about -18 to -23‰ and estuarine sediments range from -26 to -23‰ (Hedges and Mann, 1979; Jaffé et al., 2001; Wilson et al., 2005; Cifuentes, 1991; Mishima et al., 1999). Furthermore, surface sediments from the marine influenced section of Osaka Bay, Japan report $\delta^{13}C$ of -20 to -21‰ (Mishima et al., 1999). In this current study the $\delta^{13}C$ values of the sand unit are slightly more depleted in ^{13}C (negative) than that expected for sediment hosting purely marine-derived organic matter, but remain 4‰ higher than the underlying soil. The TOC values of Trench 31 show a similar sharp contrast between the underlying soil and overlying tsunami deposit. However the greatest $\delta^{13}C$ change is associated with the transition to the mud cap ($\delta^{13}C$ = 26.3‰ to -15.1‰). The positive values may result from sediment containing organic matter from plants utilising the C_4 photosynthetic pathway (range -17 to -9‰; Deines, 1980). Alternatively, the organic matter is sourced from either marine algae (-16 to -24‰), marine plankton (-13 to -31‰), marine particulate organic carbon (-18 to -24 ‰), marine bacteria (-12 to -26‰), sea grasses (marine C_4 plant) (-14 to -19‰), or possibly cyanobacteria (Deines, 1980; Tyson, 1995).

5.4 Comparison of the Tōhoku-oki and Jōgan tsunami deposits

Historical records mention several tsunamis that have impacted northeast Japan (Minoura and Nakaya, 1991; Minoura et al., 2001) however, the A.D. 869 Jōgan tsunami has been shown to be most similar to the Tōhoku-oki event in terms of the extent of inundation (Sawai et al., 2008a; Goto et al., 2011). Both tsunamis deposited a laterally extensive, landward thinning sand-sheet that extended to distances greater than 2 km from the coast (Minoura et al., 2001).

Grain size distributions were effective in discriminating the sand-sheets (medium sand) deposited by both the Tōhoku-oki and Jōgan tsunamis from the finer soils. The Jōgan sand-sheet (mean = 1.6□ ± 0.0) could be distinguished from the underlying basal soil (mean = 2.1□ ± 0.3) and overlying Towada-a tephra (mean = 2.6□) even though contacts were gradational, indicating more bioturbation. Both tsunami deposits consisted of very poorly-sorted (Tōhoku-oki: 2.0□ ± 0.3; Jōgan: 3.0□ ± 0.1) medium sand (Tōhoku-oki: 1.4□ ± 0.2; Jōgan: 1.6□ ± 0.0) that fined upwards (Tōhoku-oki trench 12: 0.5□ to 1.2□; Jōgan: 1.5□ to 1.6 □). Notable differences between the deposits include the absence of a mud cap and laminae in the Jōgan deposit. This may be evidence of post-depositional change whereby, bioturbation obscures internal structures. Szczucinski (2011) examined post-depositional changes within sediments deposited by the 2004 Indian Ocean tsunami and found significant post-depositional change only five years after the event.

The recent and fossil foraminifera also showed broad similarities and noticeable differences. Foraminifera were more abundant within the Tōhoku-oki and Jōgan tsunami deposits although bioturbation resulted in their occurrence in the underlying soil, and in the case of Jōgan, also the overlying units. The contamination of foraminifera in these units was greater in the Jōgan sequence, reflecting the gradational versus abrupt lithological contacts. In the Jōgan tsunami deposit concentrations of fossil and recent individuals were similar (recent = 190 ± 2 individuals per cm^3; fossil = 162 ± 5 individuals per cm^3), which is in contrast to the Tōhoku-oki deposit where fossil foraminifera are more abundant. The recent assemblage of foraminifera in the Jōgan sequence was dominated by *Ammonia parkinsoniana* and miliolids, but there was a noticeable presence of planktic individuals.

6. Conclusion:

The 2011 Tōhoku-oki and A.D. 869 Jōgan tsunamis are comparable in magnitude, area of coastline impacted and landward extent and show similar trends with respect to grain size distributions, foraminiferal abundances and geochemistry ($\delta^{13}C$, TOC). Both deposits can be discriminated from underlying soil by an abrupt increase in mean grain size (medium sand) and a sudden appearance of recent and fossil foraminifera. Geochemical analysis of the Tōhoku-oki deposit ($\delta^{13}C$, TOC) revealed a sharp contact between rice field soil and the overlying tsunami unit and corroborates grain size and foraminiferal results that indicate a marine source for the sand-sheet. The lack of identifiable recent foraminifera along the Sendai transect questions the utility of traditional foraminiferal analysis; however, the added use of taphonomy (test condition, fossil specimens) helped to constrain sediment provenance and hydrodynamic regime. Tracking foraminiferal taphonomic characters laterally and vertically in trenches will be important for documenting bed geometry and distinguishing tsunami and storm deposits at Sendai, as well as other locations. A comparison of the Tōhoku-oki and Jōgan tsunami deposits suggests significant post-depositional change of the latter deposit, where a mud cap and internal sedimentary structures were absent.

Acknowledgements:

Members of the UNESCO-IOC (Intergovernmental Oceanographic Commission) team to Japan provided samples and guidance. Among them we especially thank Kazuhisa Goto and Bruce Jaffe for their involvement in executing this field survey. We also thank Daisuke Sugawara, Yuichi Nishimura and Shigehiro Fujino for their assistance while on site in Japan, Kazuhisa Goto for providing survey data and Doug Jerolmack for the use of his camsizer. C. Vane publishes with the permission of the Executive Director, British Geological Survey (NERC). The work was supported in part by UNESCO-IOC, The U.S. Geological Survey and a National Science Foundation award (EAR-0842728).

References:

Berkeley, A., Perry, C. T., Smithers, S. G., 2009. Taphonomic signatures and patterns of test degradation on tropical, intertidal benthic foraminifera. Marine Micropaleontology 73, 148-163.

Bernard, E. N., Robinson, A. R. (eds.), 2009. Tsunamis. The sea, vol. 15. Harvard University Press, Cambridge, MA, 450 pp.

Bondevick, S., Lovholt, F., Harbitz, C., Mangerud, J., Dawson, A., Svendsen, J. I., 2005. The Storegga Slide tsunami - comparing field observations with numerical observations. Marine and Petroleum Geology 22, 195-208.

Chagué-Goff, C., 2010. Chemical signatures of palaeotsunamis: A forgotten proxy? Marine Geology 271, 67-71.

Chague-Goff, C., Schneider, J., Goff, J. R., Dominey-Howes, D., Strotz, L., 2011. Expanding the proxy toolkit to help identify past events – lessons from the 2004 Indian Ocean tsunami and the 2009 South Pacific tsunami. Earth-Science Reviews doi, 10.1016/j.earscirev.2011.03.007.

Cifuentes, L.A., 1991. Spatial and temporal variations in terrestrially-derived organic matter from sediments of the Delaware Estuary. Estuaries 14, 414-429.

Cisternas, M., Atwater, B. F., Torrejon, F., Sawai, Y., Machuca, G., Lagos, M., Eipert, A., Youlton, C., Salgado, I., Kamataki, T., Shishikura, M., Rajendran, C. P., Malik, J. K., Rizal., Y., and Husni, M., 2005. Predecessors of the giant 1960 Chile earthquake. Nature 437, 404-407.

Debenay, J., Beneteau, E., Zhang, J., Stouff, V., Geslin, E., Redois, F., Fernandez-Gonzalez, M., 1998. *Ammonia beccarii* and *Ammonia tepida* (Foraminifera): morphofunctional arguments for their distinction. Marine Micropaleontology 34, 235-244.

Deines, P., 1980. The isotopic composition of reduced organic carbon. In Handbook of Environmental Isotope Geochemistry edited by P. Fritz and J. C. Fontes. Amsterdam: Elsevier, 329-426.

Donato, S.V., Reinhardt, E.G., Boyce, J.I., Pilarczyk, J.E., Jupp, B.P., 2009. Particle-size distribution of inferred tsunami deposits in Sur Lagoon, Sultanate of Oman. Marine Geology 257, 54-64.

Folk, R. L., 1974. The petrology of sedimentary rocks: Austin, TX, Hemphill Publishing Co., 182p.

Geological Survey of Japan, AIST (ed.), 2009. Seamless digital geological map of Japan 1:200,000. December 15, 2009 version. Research Information Database DB084, Geological Survey of Japan, National Institute of Advanced Industrial Science and Technology.

Goff, J., Chague-Goff, C., Nichol, S., 2001. Palaeotsunami deposits: a New Zealand perspective. Sedimentary Geology 143, 1–6.

Goff, J., Lamarche, G., Pelletier, B., Chagué-Goff, C., Strotz, L., 2011. Palaeotsunami precursors to the 2009 South Pacific tsunami in the Wallis and Futuna archipelago. Earth-Science Reviews 107, 91–106.

Goodman-Tchernov, B. N., Dey, H. W., Reinhardt, E. G., McCoy, F., Mart, Y., 2009. Tsunami waves generated by the Santorini eruption reached eastern Mediterranean shores. Geology 37, 943-946.

Goni, M.A., Eglinton, T. I, 1996. Stable carbon isotopic analyses of lignin-derived CuO oxidation products by isotope ratio monitoring gas chromatography mass spectrometry (irm-GC-MS). Organic Geochemistry 24 (6-7), 601-615.

Goni, M.A., Thomas, K.A., 2000. Sources and transformations of organic matter in surface soils and sediments from a tidal estuary (north inlet, South Carolina, USA). Estuaries 23 (4), 548-564.

Goto, K., Chagué-Goff, C., Fujino, S., Goff, J., Jaffe, B., Nishimura, Y., Richmond, B., Sugawara, D., Szczucinski, W., Tappin, D.R., Witter, R.C., Yulianto, E., 2011. New insights of tsunami hazard from the 2011 Tōhoku-oki event. Marine Geology 290, 46-50.

Hawkes, A. D., Bird, M., Cowie, S., Grundy-Warr, C., Horton, B.P., Tan Shau Hwai, A., Law, L., Macgregor, C., Nott, J., Eong Ong, J., Rigg, J., Robinson, R., Tan-Mullins, M., Tiong, T., Yasin, Z., Wan Aik, L., 2007. Sediments deposited by the 2004 Indian Ocean tsunami along the Malaysia-Thailand Peninsula. Marine Geology 242, 169-190.

Hawkes, A. D., Horton, B. P., Nelson, A. R., Vane, C. H., Sawai, Y., 2011. Coastal subsidence in Oregon, USA, during the giant Cascadia earthquake of AD 1700. Quaternary Science Reviews 30, 364-376.

Hayward, B. W., Holzmann, M., Grenfell, H. R., Pawlowski, J., Triggs, C. M., 2004. Morphological distinction of molecular types in Ammonia – towards a taxonomic revision of the world's most commonly misidentified foraminifera. Marine Micropaleontology 50, 237-271.

Hedges, J.I., Mann, D.C., 1979. The lignin geochemistry of marine sediments from the southern Washington coast. Geochimica et Cosmochimica Acta 43, 1809-1818.

Horton, B. P., Edwards, R. J., 2006. Quantifying Holocene sea level change using intertidal foraminifera: Lessons from the British Isles. Cushman Foundation for Foraminiferal Research, Special Publication 40, 97pp.

Ito, Y., Tsuji, T., Osada, Y., Kido, M., Inazu, D., Hayashi, Y., Tsushima, H., Hino, R., Fujimoto, H., 2011. Frontal wedge deformation near the source region of the 2011 Tohoku-oki earthquake. Geophysical Research Letters 38, doi, 10.1029/2011GL048355.

Jaffé, R., Mead, R., Hernandez, M.E., Peralba, M.C., DiGuida, O.A., 2001. Origin and transport of sedimentary organic matter in two subtropical estuaries: a comparative, biomarker-based study. Organic Geochemistry 32 (4), 507-526.

Jankaew, K., Atwater, B.F., Sawai, Y., Choowong, M., Charoentitirat, T., Martin, M. E., Prendergast, A., 2008. Medieval forewarning of the 2004 Indian Ocean tsunami in Thailand. Nature 455, 1228-1231.

Kelsey, H. M., Nelson, A. R., Hemphill-Haley, E., Witter, R. C., 2005. Tsunami history of an Oregon coastal lake reveals a 4600 yr record of great earthquakes on the Cascadia subduction zone. GSA Bulletin 117 (7-8), 1009-1032.

Kemp, A. C., Vane, C. H., Horton, B. P., Culver, S. J., 2010. Stable carbon isotopes as potential sea-level indicators in salt marshes, North Carolina, USA. The Holocene 20 (4), 623-636.

Koper, K. D., Hutko, A. R., Lay, T., Ammon, C. J., Kanamori, H., 2011. Frequency-dependent rupture process of the 2011 Mw 9.0 Tohoku-oki Earthquake: Comparison of short-period P wave backprojection images and broadband seismic rupture models. Earth Planets Space 63, 599-602.

Kortekaas, S., Dawson, A.G., 2007. Distinguishing tsunami and storm deposits: an example from Martinhal, SW Portugal. Sedimentary Geology 200, 208-221.

Lamb, A.L., Vane, C.H., Wilson, G.P., Rees, J.G., Moss-Hayes, V.L., 2007. Assessing δ^{13}C and C/N ratios from organic material in archived cores as Holocene sea level and palaeoenvironmental indicators in the Humber Estuary, UK. Marine Geology 244, 109-128.

Loeblich, A. R., Tappan, H., 1987. Foraminiferal Genera and their Classification. Van Nostrand Rienhold Co., New York.

Mamo, B., Strotz, L., Dominey-Howes, D., 2009. Tsunami sediments and their foraminiferal assemblages. Earth-Science Reviews 96, 263-278.

Minoura, K., Imamura, F., Sugawara, D., Kono, Y., Iwashita, T. 2001. The 869 Jogan tsunami deposit and recurrence interval of large-scale tsunami on the Pacific coast of northeast Japan. Journal of Natural Disaster Science 23, 83-88.

Minoura, K., Nakaya, S., 1991. Traces of tsunami preserved in inter-tidal lacustrine and marsh deposits: some examples from northeast Japan. Journal of Geology 99, 265–287.

Mishima, Y., Hoshika, A., Tanimoto, T., 1999. Depositional rates of terrestrial and marine organic carbon in the Osaka Bay, Seto Inland Sea, Japan determined using carbon and nitrogen stable isotope ratios in the sediment. Journal of Oceanography 55, 1-11.

Morton, R., Gelfenbaum, G., Jaffe, B., 2007. Physical criteria for distinguishing sandy tsunami and storm deposits using modern examples. Sedimentary Geology 200, 184–207.

Nanayama, F., Shigeno, K., 2004. An overview of onshore tsunami deposits in coastal lowland and our sedimentological criteria to recognize them. Memoirs of the Geological Society of Japan 58, 19-33.

Nanayama, F., Shigeno, K., 2006. Inflow and outflow facies from the 1993 tsunami in southwest Hokkaido. Sedimentary Geology 187, 139-158.

Okahashi, H., Akimoto, K., Mitamura, M., Hirose, K., Yasuhara, M., Yoshikawa, S., 2002. Event deposits found in coastal marsh in Osatsu, Toba, central Japan. Chikyu Monthly 24, 698-703.

Pilarczyk, J.E., Reinhardt, E.G., 2011. Homotrema rubrum (Lamarck) taphonomy as an overwash indicator in marine ponds on Anegada, British Virgin Islands. Natural Hazards doi, 10.1007/s11069-010-9706-3.

Pilarczyk, J.E., Reinhardt, E.G., 2012. Testing foraminiferal taphonomy as a tsunami indicator in a shallow arid system lagoon: Sur, Sultanate of Oman. Marine Geology doi, 10.1016/j.margeo.2011.12.002.

Pilarczyk, J.E., Reinhardt, E.G., Boyce, J.I., Schwarcz, H.P., Donato, S.V., 2011. Assessing surficial foraminiferal distributions as an overwash indicator in Sur Lagoon, Sultanate of Oman. Marine Micropaleontology 80, 62-73.

Pinegina, T. K., Bourgeois, J., Bazanova, L. I., Melekestsev, I. V., Braitseva, O. A., 2003. A millennial-scale record of Holocene tsunamis on the Kronotskiy Bay coast, Kamchatka, Russia. Quaternary Research 59, 36-47.

Saito, Y. 1991. In: MacDonald, D. I. M., (Ed.), Sequence stratigraphy on the shelf and upper slope in response to the latest Pleistocene-Holocene sea-level changes off Sendai, northeast Japan, Sedimentation, Tectonics and Eustacy, Sequence Stratigraphy. International Assocaition of Sedimentologists Special Publication 12, 133-150.

Satake, K., Namegaya, Y., Yamaki, S., 2008. Numerical simulation of the A. D. 869 Jogan tsunami in Ishinomaki and Sendai Plains. Annual Report of Active Fault and Paleoearthquake Research 8, 71-89.

Sambridge, M., Braun, J., McQueen, H., 1995. Geophysical parametrization and interpolation of irregular data using natural neighbors. Geophysical Journal International 122, 837-857

Sato, M., Ishikawa, T., Ujihara, N., Yoshida, S., Fujita, M., Mochizuki, M., Asada, A. 2011. Displacement above the hypocenter of the 2011 Tohoku-oki earthquake. Science 332, 1395.

Sawai, Y., 2002. Evidence for 17th-century tsunamis generated on the Kuril–Kamchatka subduction zone, Lake Tokotan,Hokkaido, Japan. Journal of Asian Earth Sciences 20, 903–911.

Sawai, Y., Fujii, Y., Fujiwara, O., Kamataki, T., Komatsubara, J., Okamura,Y., Satake, K., Shishikura. M., 2008a. Marine incursions of the past 1500 years and evidence of tsunamis at Suijin-numa, a coastal lake facing the Japan Trench. The Holocene 18, 517-528.

Sawai, Y., Shishikura, M., Komatsubara, J., 2008b. A study of paleotsunami using had corer in Sendai plain (Sendai City, Natori City, Iwanuma City, Watari Town, Yamamoto Town), Miyagi, Japan. Annual Report of Active Fault and Paleoearthquake Researches 8, 17-70 (in Japanese with English abstract).

Sugawara, D., Goto, K., Chagué-Goff, C., Fujino, S., Goff, J., Jaffe, B., Nishimura, Y., Richmond, B., Szczucinki, W., Tappin, D.R., Witter, R., Yulianto, E. 2011a. Initial field survey report of the 2011 East Japan Tsunami in Sendai, Natori and Iwanuma cities. UNESCO-IOC International Tsuanmi Survey Team. 16 p.

Sugawara, D., Imamura, F., 2010. Geological and historical traces of the 869 Jogan tsunami Field Guide of Half-day Field Trip in Sendai. The 3rd International Tsunami Field Symposium, Sendai, Sanriku and Okinawa, 10-16 April 2010.

Sugawara, D., Imamura, F., Matsumoto, H., Goto, K., Minoura, K. 2011b. Reconstruction of the AD 869 Jogan earthquake induced tsunami by using the geological data. Journal of Japanese Society of Natural Disaster Science 29, 501-516.

Szczucinski, W., 2011. The post-depositional changes of the onshore 2004 tsunami deposits on the Andaman Sea coast of Thailand. Natural Hazards doi, 10.1007/s11069-011-9956-8.

Szczucinski, W., Kokocinski, M., Rzeszewski, M., Chagué-Goff, C., Cachao, M., Goto, K., Sugawara, D., this volume. Diatom assemblages and sediment grain size of 2011 Tohoku tsunami deposits near Sendai, Japan: implications for sediment sources, transport and sedimentation mode. Sedimentary Geology, this volume.

Takata, H., Takayasu, K., Hasegawa, S., 2006. Foraminifera in an organic-rich, brackish-water lagoon, Lake Saroma, Hokkaido, Japan. Journal of Foraminiferal Research 36, 44-60.

Tamura, T., Masuda, F., 2004. Inner shelf to shoreface depositional sequence in the Sendai coastal prism, Pacific coast of northeastern Japan: spatial and temporal growth patterns in relation to Holocene relative sea-level change. Journal of Asian Earth Sciences 23, 567-576.

Tamura, T., Masuda, F., 2005. Bed thickness characteristics of inner-shelf storm deposits associated with a transgressive to regressive Holocene wave-dominated shelf, Sendai coastal plain, Japan. Sedimentology 52, 1375-1395.

Tyson, R.V., 1995. Sedimentary Organic Matter: organic facies and palynofacies. London: Chapman Hall.

Uchida, J., Fujiwara, O., Hasegawa, S., Kamataki, T., 2010. Sources and depositional processes of tsunami deposits: Analysis using foraminiferal tests and hydrodynamic verification. Island Arc 19, 427-442.

Vane, C.H., Drage, T.C., Snape, C.E., 2003. Biodegradation of Oak (Quercus alba) wood during growth of the shiitake mushroom (lentinula edodes): A molecular approach. Journal of Agricultural and Food Chemistry 51, 947-956.

Vane, C.H., Kim, A.W., McGowan, S., Leng, M.J., Heaton, T.H.E., Kendrick, C.P., Coombs, P., Yang, H., Swann, G.E.A., 2010. Sedimentary records of sewage pollution using faecal markers in contrasting peri-urban shallow lakes. Science of The Total Environment 409 (2), 345-356.

Wilson, G.P., Lamb, A.L., Leng, M.J., Gonzalez, S., Huddart, D., 2005. $\delta^{13}C$ and C/N as potential coastal palaeoenvironmental indicators in the Meresy Estuary, UK. Quaternary Science Reviews 24, 2015-2029.

Yamada, I., Shoji, S., 1981. The Late Holocene felsic tephra in Miyagi Prefecture. Journal of the Pedological Society of Japan 52, 155-158.

Zhao, D., Horiuchi, S., Hasegawa, S., 1990. 3-D seismic velocity structure of the crust and the uppermost mantle in the northeastern Japan arc. Tectonophysics 181, 135-149.

Figure captions:

Fig. 1: a) Map of Sendai, Japan showing broad-scale tectonics. The inferred fault zone rupture segmentation (purple ellipse) and the epicenter (black square) of the Tōhoku-oki earthquake are indicated (after Koper et al., 2011) along with the estimated source region of the A.D. 869 Jōgan tsunami (after Minoura et al., 2001). Location of trench transect (inset) and Jōgan trench (white circle) are indicated. **b)** Detailed map of study area showing site locations of Tōhoku-oki trenches and surface samples (site 1 – 4).

Fig. 2: a) Remnants of the artificial dune after the Tōhoku-oki tsunami. The tsunami breached the dune in several locations and flattened pine trees and coastal shrubs, exposing an underlying stabilizing net. b) Tsunami-flattened coastal forest planted ~300 years ago to shelter rice fields from wind and salt spray. Large pine trees were flattened in a shore-normal direction, and in some cases uprooted, as a result of the tsunami. **c)** Tōhoku-oki deposit at Trench 31 (see Fig. 1b) indicating a ~10 cm thick sand unit with a mud cap overlying basal rice field soil.

Fig. 3: Surface samples (red) compared to changes in the Tōhoku-oki deposit (blue) with increasing distance inland. **a)** Elevation along a transect from the nearshore Pacific ocean through the coastal forest, paved landscape and rice fields using the Tokyo Peil datum (TP; mean sea level in Tokyo Bay; see Fig. 1a,b). **b-d)** Total concentration and relative abundances of foraminiferal taphonomic data. **e-h)** Average mean (**e**), mode

(**f**), standard deviation (sorting; **g**), and degree of angularity (sphericity; **h**) data for Tōhoku-oki trenches. **i)** Tsunami deposit thickness. **j)** Average particle size distribution (PSD) plot.

Fig. 4: a) Core Average particle size distribution (PSD) plots for Tōhoku-oki trench sections along a transect. Facies designations are based on field observations and black dots represent sampling intervals. **b)** Generalized stratigraphic section of the Tōhoku-oki tsunami deposit based on all trench sections. **c)** Core PSD plot for the Jōgan trench section (Fig. 1a). **d)** Generalized stratigraphic section of the Jōgan tsunami deposit including the overlying Towada-a tephra deposited by volcanic activity to the north of Sendai in A. D. 870 – 934. **e)** Location of trench sites. For elevation (meters above TP) and distance from the coastline see Fig. 5a.

Fig. 5: a) Grain size and foraminiferal taphonomic data for trenches 5, 12, 31, 48 and Jōgan. Geochemistry data ($\delta^{13}C$, TOC) for trenches 5 and 12 is indicated. Black dots indicate sampling intervals. b**)** Trench site locations. For elevation (m MSL) and distance from the coastline see Fig. 5a.

Fig. 6: Average particle size distribution (PSD) statistical data for facies. Surface samples representing possible sources of tsunami sand are compared with Tōhoku-oki trench sections.

Plate 1: All scale bars are equal to 100 µm. 1 – 2. Light microscope images of sediment in-filled fossil specimens. 3 – 4. SEM images of fossil specimens indicating highly corroded and abraded tests. 5. Recent *Ammonia parkinsoniana* ventral view. 6. Recent *Ammonia parkinsoniana* dorsal view. 7 – 10. Taphonomically altered (corroded, abraded, edge rounded) recent miliolids.

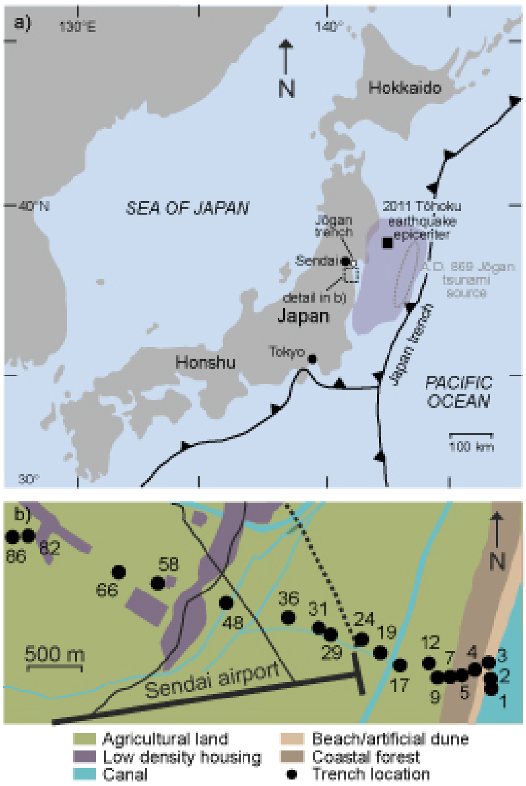
a)
130°E
140°
40°N
30°
N
Hokkaido
SEA OF JAPAN
2011 Tōhoku earthquake epicenter
Jōgan trench
Sendai
A.D. 869 Jōgan tsunami source
detail in b)
Japan
Honshu
Tokyo
Japan trench
PACIFIC OCEAN
100 km
b)
86
82
66
58
48
36
31
29
24
19
17
12
9
7
5
4
3
2
1
N
500 m
Sendai airport
Agricultural land
Low density housing
Canal
Beach/artificial dune
Coastal forest
Trench location

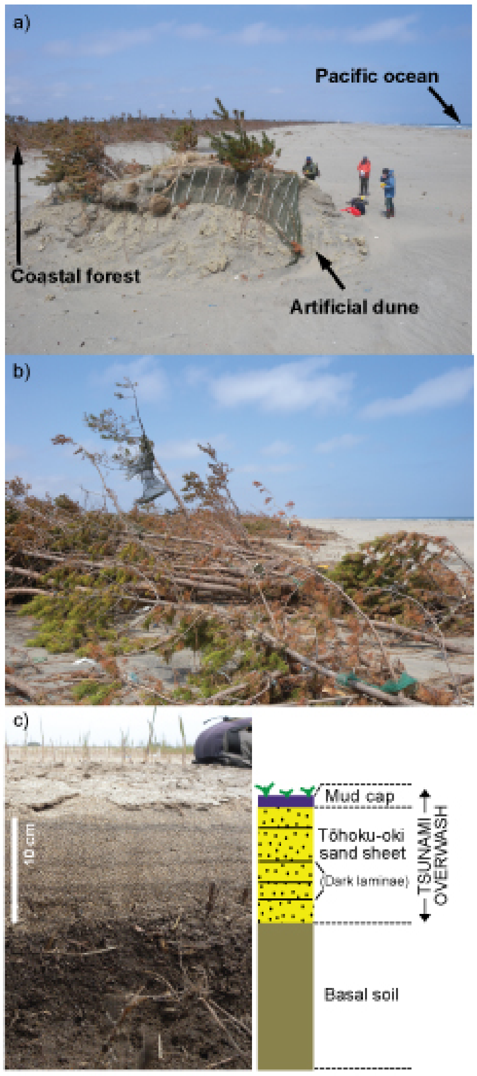
a)
Pacific ocean
Coastal forest
Artificial dune
b)
c)
10 cm
Mud cap
Tōhoku-oki sand sheet
(Dark laminae)
TSUNAMI OVERWASH
Basal soil

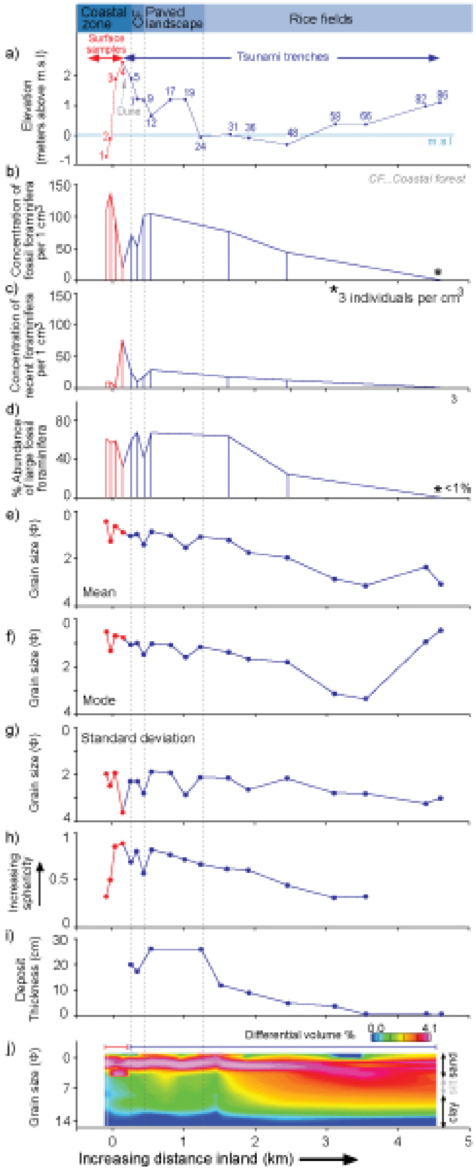
Coastal zone
CF
Paved landscape
Rice fields
a)
Surface samples
Tsunami trenches
Elevation (meters above m.s.l.)
1
2
3
4
5
7
9
12
17
19
24
31
36
48
58
66
82
86
Dune
m.s.l.
b)
Concentration of fossil foraminifera per 1 cm3
CF...Coastal forest
*3 individuals per cm3
c)
Concentration of recent foraminifera per 1 cm3
d)
% Abundance of large fossil foraminifera
* <1%
e)
Grain size (Φ)
Mean
f)
Grain size (Φ)
Mode
g)
Grain size (Φ)
Standard deviation
h)
Increasing sphericity
i)
Deposit Thickness (cm)
j)
Grain size (Φ)
Differential volume %
0.0
4.1
sand
silt
clay
Increasing distance inland (km)
0
1
2
3
4
5

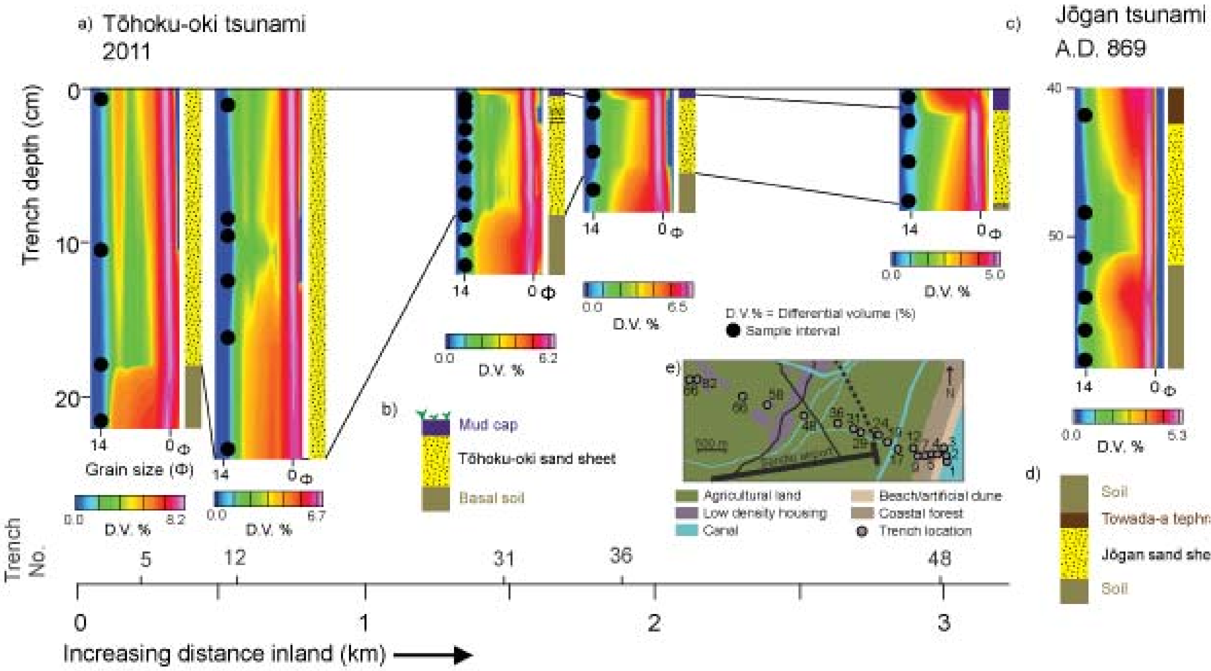
a) Tōhoku-oki tsunami 2011
c) Jōgan tsunami A.D. 869
Trench depth (cm)
0
10
20
40
50
14
0 Φ
Grain size (Φ)
0.0
8.2
6.7
6.2
6.5
5.0
5.3
D.V. %
D.V.% = Differential volume (%)
● Sample interval
b)
Mud cap
Tōhoku-oki sand sheet
Basal soil
d)
Soil
Towada-a tephr
Jōgan sand she
Soil
e)
N
100 m
Agricultural land
Low density housing
Canal
Beach/artificial dune
Coastal forest
Trench location
Trench No.
5
12
31
36
48
0
1
2
3
Increasing distance inland (km)

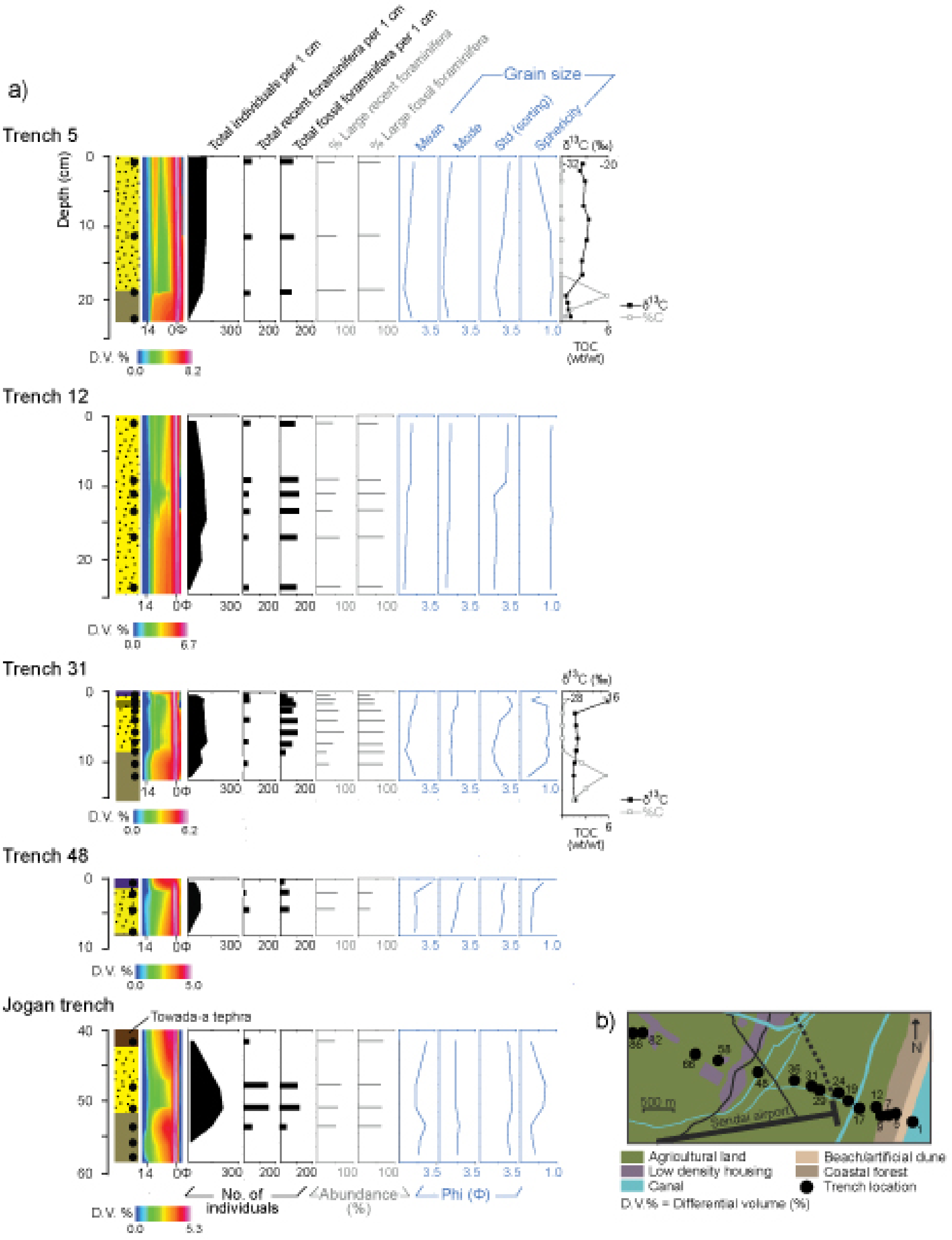a)
Total individuals per 1 cm
Total recent foraminifera per 1 cm
Total fossil foraminifera per 1 cm
% Large recent foraminifera
% Large fossil foraminifera
Grain size
Mean
Mode
Std (sorting)
Sphericity
Trench 5
Depth (cm)
0
10
20
14
0Φ
300
200
200
100
100
3.5
3.5
3.5
1.0
$\delta^{13}C$ (‰)
-32
-20
$\delta^{13}C$
%C
6
TOC (wt/wt)
D.V. %
0.0
8.2
Trench 12
D.V. %
0.0
6.7
Trench 31
-28
-16
D.V. %
0.0
6.2
Trench 48
D.V. %
0.0
5.0
Jogan trench
Towada-a tephra
40
50
60
No. of individuals
Abundance (%)
Phi (Φ)
D.V. %
0.0
5.3
b)
N
500 m
Sendai airport
86
82
66
58
48
36
31
29
24
19
17
12
7
8
5
1
Agricultural land
Low density housing
Canal
Beach/artificial dune
Coastal forest
Trench location
D.V.% = Differential volume (%)

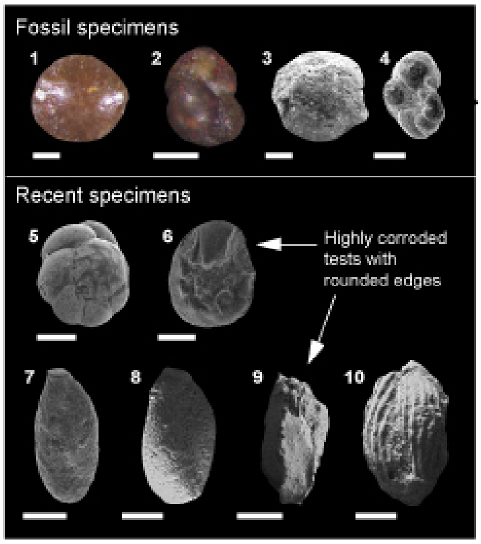
Fossil specimens
1
2
3
4
Recent specimens
5
6
Highly corroded tests with rounded edges
7
8
9
10